A major purpose of the Technical Information Center is to provide the broadest dissemination possible of information contained in DOE's Research and Development Reports to business, industry, the academic community, and federal, state and local governments.

Although a small portion of this report is not reproducible, it is being made available to expedite the availability of information on the research discussed herein.

CONF-830805--2

LA-UR -83-391

LA-UR--83-391

DE83 007553

Los Alamos National Laboratory is operated by the University of California for the United States Department of Energy under contract W-7405-ENG-36

TITLE THERMO-STRUCTURAL INVESTIGATION OF THE FORT ST. VRAIN REACTOR UNDER OPERATING AND UPSET CONDITIONS

AUTHOR(S) Charles A. Anderson, Karl L. Meier, Deborah R. Bennett

SUBMITTED TO SMiRT Conference
Mme J. Stalpaert
Commison of the European Communities
DG XIII - A-3 - Groupe de Liaison
MDB 4/28
200, rue de La Loi
B-1049 Brussels Belgium

NOTICE

PORTIONS OF THIS REPORT ARE ILLEGIBLE. It has been reproduced from the best available copy to permit the broadest possible availability.

DISCLAIMER

This report was prepared as an account of work sponsored by an agency of the United States Government. Neither the United States Government nor any agency thereof, nor any of their employees, makes any warranty, express or implied, or assumes any legal liability or responsibility for the accuracy, completeness, or usefulness of any information, apparatus, product, or process disclosed, or represents that its use would not infringe privately owned rights. Reference herein to any specific commercial product, process, or service by trade name, trademark, manufacturer, or otherwise does not necessarily constitute or imply its endorsement, recommendation, or favoring by the United States Government or any agency thereof. The views and opinions of authors expressed herein do not necessarily state or reflect those of the United States Government or any agency thereof.

By acceptance of this article, the publisher recognizes that the U.S. Government retains a nonexclusive, royalty-free license to publish or reproduce the published form of this contribution, or to allow others to do so, for U.S. Government purposes.
The Los Alamos National Laboratory requests that the publisher identify this article as work performed under the auspices of the U.S. Department of Energy.

MASTER

Los Alamos Los Alamos National Laboratory
Los Alamos, New Mexico 87545

FORM NO 836 R4

THERMO-STRUCTURAL INVESTIGATIONS OF THE FORT ST. VRAIN REACTOR UNDER OPERATING AND UPSET CONDITIONS *

Charles A. Anderson, Karl L. Meier, and Deboran R. Bennett
Los Alamos National Laboratory
Los Alamos, New Mexico

ABSTRACT

This paper summarizes the results of tnree tnermo-structural investigations of the behavior of the Fort St. Vrain reactor under operating and upset conditions. Tne Fort St. Vrain (FSV) reactor is a 330 Mwe High Temperature Gas-Cooled Reactor operated by tne Public Service Company of Colorado (PSCo). The tnree investigations are concerned witn liner cooling system hot spots, with control rod drive mechanism over temperature, and with structural integrity of the core support under a postulated loss-of-flow condition.

Seven hot spot areas have been identified in tne FSV Prestressed Concrete Reactor Vessel (PCRV) Liner Cooling System, which exceed the Final Safety Analysis Report (FSAR) hot spot temperature criteria of 200°F at the concrete/liner interface under normal operating conditions. The PCRV is protected from the circulating helium coolant by a tnermal barrier lining the PCRV interior, and tne liner cooling system, a system of water-cooled tubes welded to the concrete side of the liner. Discontinuities in tne thermal barrier and higher than anticipated heat loads produce increased concrete temperatures at tne liner/concrete interface. Localized conditions are used in evaluating each of tne hot spot areas with finite element models.

During reactor rise-to-power testing, tne Control Rod Drive Mechanism (CRDM) motor temperatures were measured as nign as 226°F at 83% reactor power. These temperatures were appreciably above those predicted for tne CRDM and were also above tne qualification test temperature. Tne cause of overheating is ingress of hot primary nelium into tne refueling penetration, flowing up to tne Orifice Valve Motor (OVM) support plate and tnrougn tne OVM plate into the CRDM cavity. A thermal model calculated CRDM temperatures wnicn agreed quite well with the temperatures measured during reactor testing.

A postulated accident condition is considered in the tnermoelastic stress analysis of a FSV graphite core support block. The support block is subjected to thermal stresses caused by a loss of forced circulation (LOFC) accident of the reactor system, followed by restoration of partial cooling. Two and tnree-dimensional finite element models of the core support block were analyzed for thermal stresses, and gave results that verify tne integrity of this structural component under the given accident conditions.

*This work was supported by the Division of Licensing of the United States Nuclear Regulatory Commission.

1. EVALUATING THE SEVERITY OF THE FORT ST. VRAIN PCRV LINER HOT SPOTS

1.1. Introduction

The primary objectives of this study were to review the data for the FSV Prestressed Concrete Reactor Vessel (PCRV) Liner Cooling System hot spot areas, to determine the temperature distribution at the PCRV liner/concrete interface for each area, and to evaluate the severity and consequences of the hot spots on reactor safety and performance.

The seven localized PCRV liner cooling system hot spots can be identified in Fig. 1 as:

- the core support floor region beneath the core barrel support structure;
- the loop divider baffle intersection with the PCRV bottom head liner, side walls, and lower access penetration;
- the helium purification train crossover pipe intersection with the high temperature filter absorber (HTFA) penetration in the PCRV top head;
- the core outlet thermometer penetrations in the PCRV sidewall;
- the refueling penetrations in the PCRV top head;
- the peripheral seal at the edge of the lower floor; and
- the steam generator penetration intersection with the PCRV bottom head.

As cited in the FSV Final Safety Analysis Report (FSAR,), [1] Sec. 5.9, the safe operation of the PCRV is dependent on strict control of its thermal environment at all times. The PCRV is protected from the principal source of potentially damaging heat, the primary helium coolant, by the thermal barrier and the liner cooling system. The thermal barrier consists of ceramic insulation blankets compressed against the helium side of the PCRV liner by steel plates. Heat passing through the thermal barrier to the liner is removed by the liner cooling system. This system is composed of two independent cooling loops, each loop consisting of water-cooled tubes (1 $in.^2$) continuously welded to the concrete side of the liner in an alternate tube/alternate loop manner. A cross-sectional schematic of the cooling tube/liner interface configuration is shown in Fig. 2.

The heat load to the liner cooling system is dominated by the heat transfer across the thermal barrier, and is a direct function of the difference between the inlet gas temperature (~750°F at 100% power) and the liner cooling system average water temperature (~110°F). The heat load is directly proportional to reactor power.

1.2. Defining a Hot Spot and Its Causes

Under normal operating conditions, the thermal barrier and liner cooling system maintain the the design temperature distribution in the PCRV according to the following criteria:

- the bulk concrete shall have an effective temperature of 130°F,
- the local maximum concrete temperature shall be 150°F, midway between cooling tubes at the liner/concrete interface, and
- the liner cooling water differential temperature shall not exceed 20°F.

However, a hot spot is defined in the FSAR as an area having a local maximum concrete temperature of 200°F or greater, under normal operating conditions, and 250° with only one cooling loop in operation. In addition, Amendment 29 to the FSAR stipulates that, in the core support floor under the barrel support pad, the cooling water differential temperature may be 40°F, and the local maximum concrete temperature may reach 250°F under normal operating condition, and 360°F with one cooling loop in operation.

The liner hot spot areas are generally caused by a discontinuity in the thermal barrier, providing a lower resistance path between the heated helium and the liner/concrete interface. Structural attachments to the liner also provide a direct heat conduction path to the liner. Higher than expected heat fluxes can also be caused by bypass or impinging helium flow patterns, or by unsuitable cooling tube configuratons. In either case, the result is the same--the liner cooling system is unable to maintain the concrete temperature distribution within design limits.

1.3. Hot Spot Modeling

In the liner cooling system analysis we first calculated the general effect of the cooling tube on the localized concrete temperature distribution, using the finite element code TSAAS (Ref. [2]). This initial parametric study evaluated the effects of tube pitch, cooling water heat transfer coefficient and temperature, and the thermal flux to the liner, which is in turn a function of geometry and of helium flow rate, temperature and pressure for given reactor power conditions. The temperature distribution and local maximum concrete temperature for a given hot spot area were then calculated. Finite element models were developed for each hot spot, based on the local geometric and heat transfer conditions. A characterization of the local fluid flow patterns allowed heat transfer coefficients to be calculated using classic correlations, thereby producing a set of "worst case" boundary conditions to act as an analytical upper bound. Lower power cases were run prior to 100% power conditions, in order to compare existing data to derived results in model verification. A typical finite element model for the core support floor periphery is shown in Fig. 3, together with computed temperature contours.

1.4. Conclusions

To varying degrees of temperature and affected concrete volume, all seven hot spot areas exceed the 200° local maximum concrete temperature limit imposed by the FSAR. However, the temperature limit alone is not an adequate determination of the severity of each hot spot area as the load carrying capability of concrete at elevated temperatures is a function of temperature, the volume of concrete affected by the elevated temperatures, and the applied stress. Therefore, we have initiated the development of an acceptance criterion for the PCRV liner cooling system hot spots, based on varying degrees of severity and requiring justification and/or corrective action for hot spot acceptability.

2. FORT ST. VRAIN CONTROL ROD DRIVE MECHANISM OVER TEMPERATURE INVESTIGATION

2.1 Introduction

The Fort St. Vrain reactor has 37 refueling regions, each containing a control rod drive mechanism (CRDM), which serves to retract, and hold stationary, two control rods during reactor operation. The CRDMs release and allow the rods to fall by gravity into the core during shutdown. The mechanism, as shown in Fig. 4, consists of an electric motor which turns a drum winding up the cables attached to the control rods. A set of pulleys guides the two cables onto the drum and an electric brake holds the drum stationary when the motor is de-energized. The CRDM is enclosed at the upper end of the refueling penetration in a cavity that is filled by a purge flow from the helium purification system.

Because proper operation of the CRDM is critical for reliable safe operation of the reactor, a series of qualification tests was conducted on the CRDM to demonstrate its

capability. Over a one year time span, the CRDM was non-continuously tested in a 180°F helium environment. The CRDM motor temperatures during these tests varied between 200-230°F, and averaged 215°F.[3] Maximum temperatures were found on the CRDM motor because of the dissipated electrical power.

Reactor rise-to-power tests conducted in 1977-78 at power levels up to 70% produced motor temperatures up to 213°F, which was several degrees hotter than anticipated. Then, as now, the fundamental cause of overheating of the CRDM and the PCRV in this region appeared to be ingress of primary helium into the refueling penetration and its flow up to the orifice valve motor (OVM) plate. A small amount of this helium apparently leaked into the CRDM cavity through penetrations in the OVM plate. Subsequent seal replacement helped to reduce this helium inleakage.

Later, during reactor tests between 1978 and 1981, temperatures were monitored in the CRDM cavities of five reactor regions by thermocouples installed at several locations in the cavities. The maximum CRDM temperature measured during these tests was 226°.

2.2 Temperature Data

Temperature data for the instrumented CRDMs were supplied by the reactor operator, PSCo, and spanned the time from startup in 1975 to November 7, 1981, with reactor power levels from a few percent to 100%. A compendium of CRDM motor temperature data for pre-1981 tests is given in Fig. 5, for power levels less than 70%. Data from 1981 reactor tests in the range of 70-100% power are also included in Fig. 5. CRDM motor temperatures are shown for orifice valve openings greater than 40%, except for the area delineated by the box that shows data for orifice valve openings less than 15%. Small orifice valve openings raise the differential pressure between primary helium and the orifice valve assembly, resulting in increased flow of hot primary helium into the CRDM region. Maintaining the orifice valve opening at a minimum of 40% means that the motor temperature does not exceed the average qualification test temperature of 215°F at full power.

2.3 Thermal Analysis

A thermal analysis of the CRDM and environs was made to better understand the over-temperature problem and to seek ways of mitigating it, using the heat transfer computer code TRUMP. The elements of the calculational model are shown in Fig. 6. The model extends vertically from the OVM plate upward through the CRDM cavity to the missile plate and ambient air. Horizontally, the model extends from the CRDM centerline radially through the cavity liner to the PCRV concrete. Helium in the CRDM cavity flows in a natural convection loop downward at the liner and upward from the OVM past the CRDM. A purified helium purge flow enters at the secondary closure plate and joins the natural convection stream. Hot primary helium in-leakage can occur through the OVM plate fittings, join the convection stream, and flow upward past the CRDM. Unfortunately, this natural convection pattern is disadvantageous in minimizing the CRDM temperature.

In the model, heat is removed from the CRDM region by the water-cooled PCRV, the ambient air, and the helium purge flow. Heat enters the region via convection and radiation from the OVM and OVM plate. Heat also enters via the brake electrical losses, hot helium in-leakage and conduction up the control cables. TRUMP thermal analysis results are shown in Table I for several cases. The Base Case (Case 1) assumes the following--4 lb/hr helium purge flow at 100°F, no hot helium in-leakage, 100°F ambient air, PCRV concrete temperatures of 130°F and 122°F, and OVM plate temperatures of 271°F as measured

during the 100% reactor power test. The analysis predicts the CRDM motor temperature as 199°F as shown in Table I.

If 2 lb/hr of primary helium in-leakage is added to the convection stream at the OVM plate temperature (Case 5), the CRDM maximum motor temperature rises to 212°F as shown in in the thermal analysis results of Fig. 6. This case predicts temperatures very close to those measured in full power tests. However, several methods are available for mitigating the CRDM temperature and were studied with the numerical model. Doubling the helium purge flow to 8 lb/hr at 100°F (Case 2) reduces the corresponding temperature in the CRDM by 8°F, resulting in a 2°F reduction per lb/hr of additional purge flow. Cooling the normal purge flow from 100°F to 60°F reduced the CRDM temperature 7°F as shown in Case 3. Judiciously applied reflective coatings on the OVM and OVM plate reduce their thermal input and can result in reducing motor temperatures by 24°F (Case 8). A thin insulating layer applied to the underside of the OVM plate can be instrumental in reducing CRDM temperature by 33°F (Case 9). By both reflective coating and insulating the top of the OVM and OVM plate, a combined temperature reduction of 37°F is obtained as shown in Case 10. Reversing the natural convection flow loop inside the CRDM cavity with a baffling system (Case 4) can reduce the temperature 11°F from the base case.

2.4 CONCLUSIONS

By using a modern calculational tool, we have been able to quantify the CRDM overtemperature problem. It appears that CRDM temperature levels can be controlled with appropriate orifice valve openings and can be mitigated by the numerous methods analyzed above.

3. THREE-DIMENSIONAL THERMOELASTIC ANALYSIS OF A FORT ST. VRAIN CORE SUPPORT BLOCK

3.1 Introduction

During the cooldown following a loss of forced circulation (LOFC) accident in the Fort St. Vrain High-Temperature Gas-Cooled Reactor, thermal stresses in the graphite core support blocks (CSBs) could conceivably exceed the minimum tensile strength of graphite. Potentially large thermal stresses are possible because of the high thermal gradients established across the core support structure during the LOFC phase of the accident and during the following period when the emergency firewater cooldown (FWCD) system partially restores forced circulation. This section summarizes an investigation of the thermal stresses that would be experienced by the CSBs during the cooldown period.

3.2 Accident Scenario

The Fort St. Vrain reactor core is helium-cooled and consists of vertical columns of graphite blocks divided into 37 fuel regions. Each region nominally consists of six fuel columns and one control column and is supported by one CSB. The CSBs are loosely keyed together (Fig. 7) to provide uniform gaps of 0.4 to 1.0 in. between adjacent CSBs, depending on the average temperature of the reactor. Figure 7 also shows the alternating lugs and keyways (three of each) on the sides of the CSB, and that each CSB is supported on the bottom by three support posts.

Core heat removal is normally accomplished by the downward flow of helium coolant through the core. At the base of the active core, the gas is channeled through the lower reflector columns into the six coolant channels of the CSB. During an LOFC accident, forced circulation of the helium is interrupted. Before it can be restored, heat is transferred within the core through conduction in the graphite and by free convection in the helium. Because the amount of power available in different regions varies significantly, large temperature gradients are established in the support structure. The

differences in temperatures between regions are compounded because in low-power regions, free convection of the helium is naturally downward, which provides a cooling effect. In high-power regions, the flow is upward, causing the temperatures to rise.

The accident scenario considered in this report assumes that helium forced circulation is partially restored by the emergency FWCD system, 90 min. into the LOFC accident. With forced circulation reinitiated, some of the CSBs initially increase in temperature as heat in the active core is forced toward the bottom of the reactor. During this time, the low-power regions are cooled more rapidly because the helium viscosity is lower and the density greater at lower temperatures. This effect accentuates the already high temperature differences between the CSBs. Numerical predictions indicate that the average temperatures of adjacent CSBs may differ by as much as 600°F during the cooldown period following the LOFC.

3.3 Method of Analysis

During cooldown, heat is transferred to or from the CSBs by the helium flowing through the coolant channels, to the helium bypass flow in gaps between CSBs, into or out of the CSBs by conduction through the reflector columns above the CSBs, to adjacent CSBs by conduction at points of contact and across the helium bypass gap, and to adjacent blocks by radiation. Less significant heat is transferred through the core support posts and by radiation and convection to the area under the CSBs.

Thermal boundary conditions for the thermal-stress solutions for an individual CSB were obtained from temperature data supplied by the Oak Ridge National Laboratory (ORNL), and were based on computations made with the ORECA computer code. Because of uncertainty concerning some of the critical parameters in the thermal solution, several parallel computations were performed to determine the sensitivity of thermal stresses to these parameters.

The CSB thermal stresses were calculated in three successive steps, using the finite element method. In the first step, two simple two-dimensional finite element models representing the top surface of a CSB (Fig. 8) were developed to perform scoping studies of the problem and to eventually help quantify the effect of asymmetries in heat flow on the stresses. The first model determined the temperature distribution in the CSB top surface, while with the second model we calculated the resulting thermal stresses.

The geometric complexity of the CSB actually requires a three-dimensional model to adequately represent the complicated heat flow patterns and associated stress fields. The CSB geometry was somewhat simplified to make the structure cyclically symmetric and to eliminate discontinuities such as keyways and lugs. The cyclic symmetry was artificially obtained by rotating the coolant hole pattern (10° 56.3') relative to the CSB boundary. The resulting finite element model is shown in Fig. 9. The ADINAT heat transfer code was then used to determine the temperature distribution within the CSB model for both transient and steady-state conditions, and provided temperature fields for a three-dimensional thermoelastic stress analysis. Figure 10 illustrates temperature contours and contours of the maximum principal stress for one of the cases studied.

The third step considered the stress concentration effects at the CSB keyway, which was not included in the larger three-dimensional analysis. By using steady-state results from the first two steps to set appropriate boundary conditions on a substructure model,

we were able to calculate maximum stresses at the CSB keyway location. Details are discussed in Ref. [4].

3.4 Conclusions

Average CSB temperature transients for an LOFC/FWCD accident calculated by ADINAT were in good agreement with ORECA temperature predictions. The maximum principal stress in the CSB calculated for a 105% power level was 915 psi at the keyway corner on the top of the CSB and includes a factor for asymmetries and a stress concentration factor of 1.8 at the keyway corner. The resulting factor of safety is 1.27, using a minimum tensile strength of 1160 psi for graphite. This factor is sufficient for these loading conditions because the thermal stresses are secondary in nature and a local failure would relieve the stresses in the CSB. Adding to the confidence level that the CSB will not fail under these conditions is the fact that the stress gradients are very high near the point of maximum stress. That is, most of the CSB remains at a much lower stress level, and any cracks that start in the high-stress region would probably arrest before propagating any significant distance. The stress levels for 72% power are approximately 60% of those for 105% power levels.

REFERENCES

[1] Final Safety Analysis Report, Fort St. Vrain Nuclear Generating Station-Unit No. 1, Public Service Co. of Colorado.

[2] R. V. Browning and C. A. Anderson, "TSAAS-Finite Element Thermal and Stress Analysis of Plane and Axisymmetric Solids with Orthotropic Temperature-Dependent Material Properties", Los Alamos National Laboratory report, LA-5599-MS (Revision 1), February, 1982.

[3] Private Communication, Public Service Company of Colorado.

[4] T. A. Butler and C. A. Anderson, "Three-Dimensional Thermoelastic Analysis of a Fort St. Vrain Core Support Block", NUREG/CR-2319, LA-9003-MS, Los Alamos National Laboratory, 1981.

TABLE I
CRDM THERMAL ANALYSIS RESULTS

Case No.	Conditions (Changed from base case)	Temperature (°F)				
		CRDM	Missile Plate	Cavity Helium	OVM	Closure Plate
1	Base case 100% power	199	128	179	262	153
2	Double purge flow (8 lb/hr)	191	126	166	261	147
3	Purge flow 4 lb/hr at 60°F	192	126	168	261	147
4	Reverse convection loop flow	188	128	145	261	151
5	In-leakage flow 2 lb/hr	212	132	203	262	162
6	In-leakage flow 2 lb/hr, reflective coating	183	127	192	273	151
7	Base case 70% power	183	126	165	233	146
8	Reflective coating on OVM, OVM plate	176	125	167	267	145
9	Insulation on under side OVM plate	166	122	152	201	139
10	Insulation and reflective coating OVM, OVM plate	162	122	147	269	139

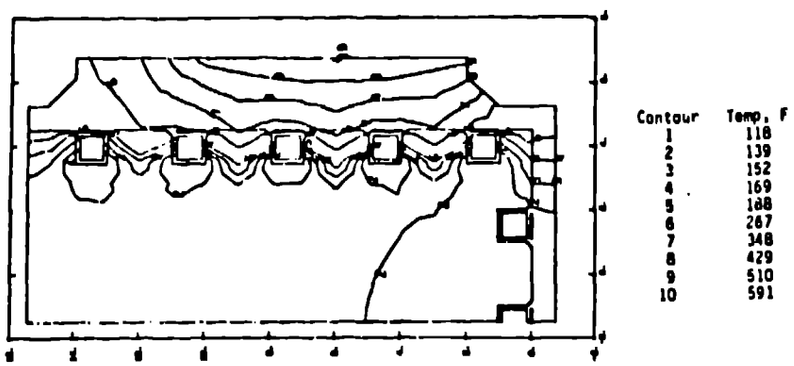

FIG. 3.8. CSF PERIPHERAL TEMPERATURE DISTRICUTION
100% POWER, 1.0% BYPASS FLOW.

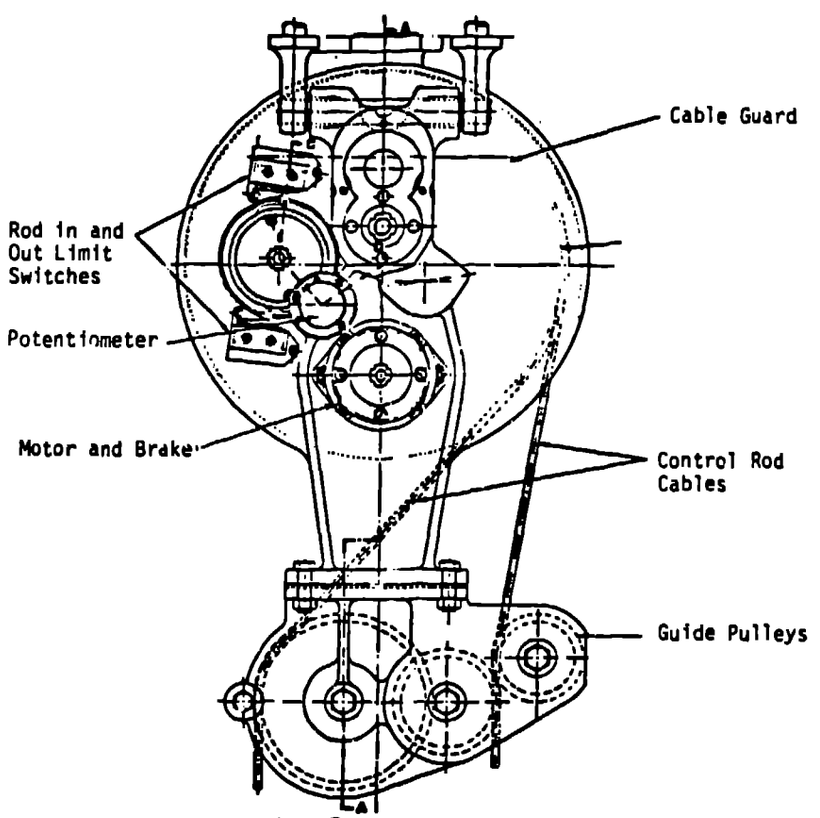

FIG. 4. CONTROL ROD DRIVE MECHANISM.

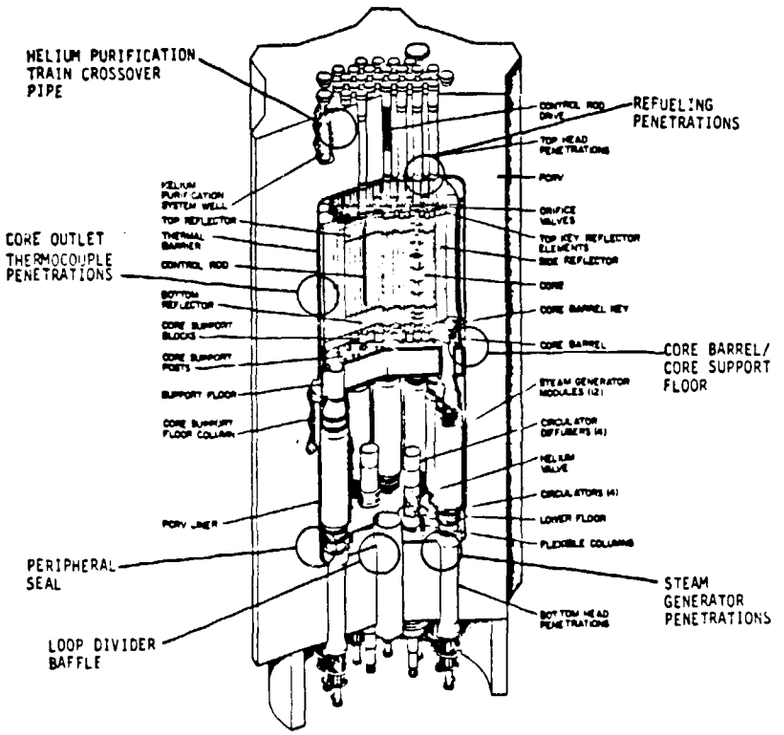

FIG. 1. FSV-PCRV LINER HOT SPOTS

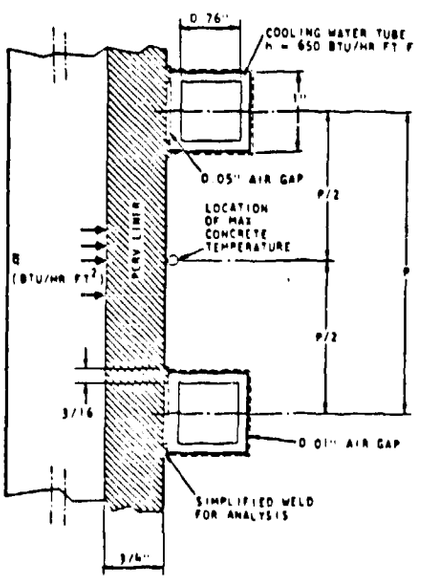

FIG. 2. PCRV LINER COOLING

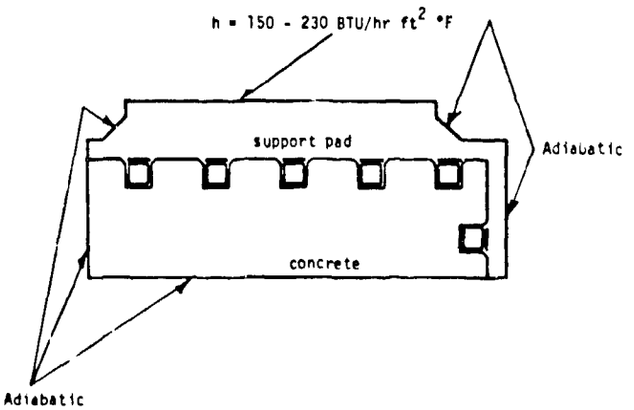

FIG. 3.A. CORE SUPPORT FLOOR (CSF) MODEL.

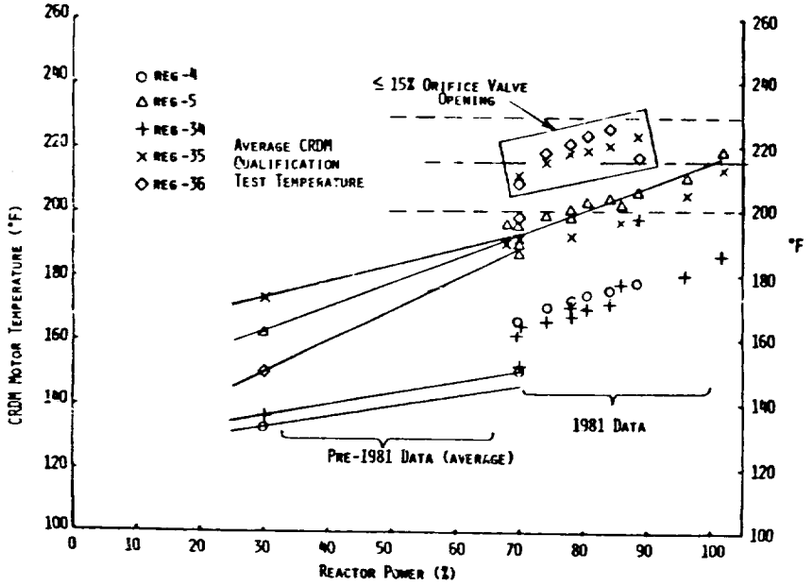

FIG. 5. CRD MOTOR TEMPERATURE VS REACTOR POWER

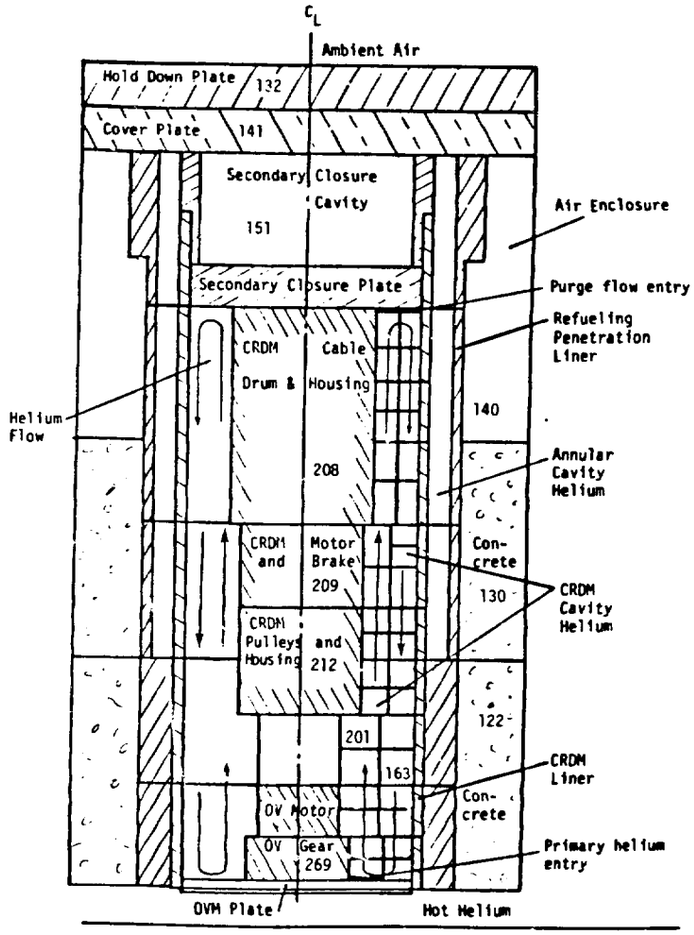

FIG. 6. CRDM THERMAL ANALYSIS MODEL.

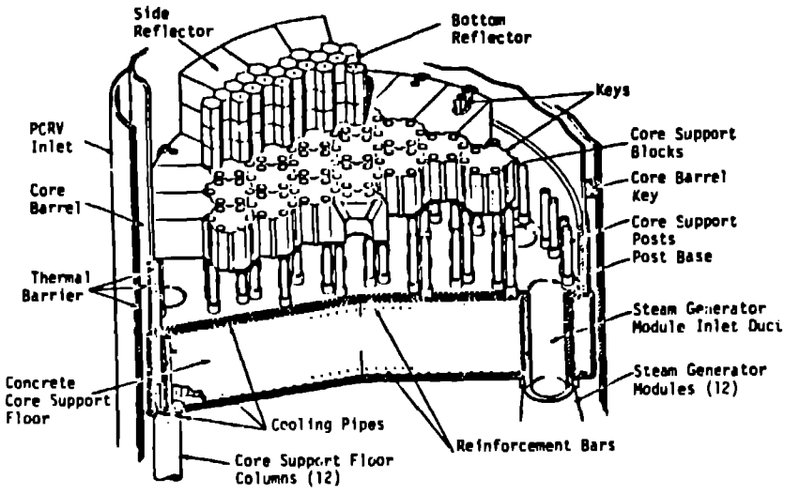

FIG. 7. CORE SUPPORT ARRANGEMENT.

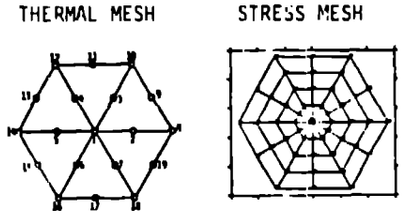

FIG. 8. MESHES FOR TWO-DIMENSIONAL FINITE ELEMENT MODELS.

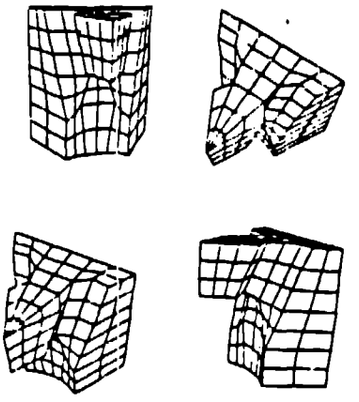

FIG. 9. MESH FOR THREE-DIMENSIONAL FINITE ELEMENT MODEL.

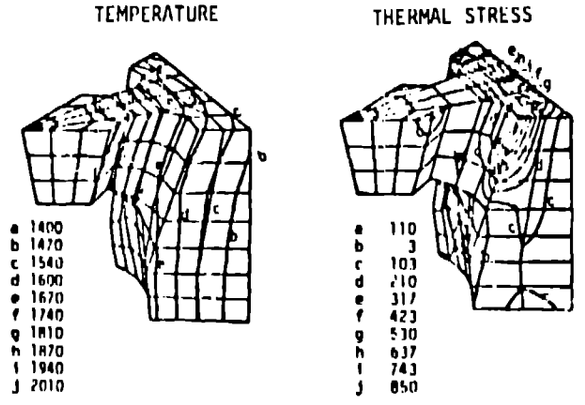

FIG. 10. TEMPERATURE AND MAXIMUM PRINCIPAL STRESS DISTRIBUTION IN CSB FOR PRELIMINARY STEADY-STATE ANALYSIS.